

# Automatic Road Segmentation of Traffic Images

Chiung-Yao Fang<sup>1</sup>, Han-Ping Chou<sup>2</sup>, Jung-Ming Wang<sup>1</sup> and Sei-Wang Chen<sup>1</sup>

<sup>1</sup>Dept. of Computer Science and Information Engineering, National Taiwan Normal University, Taipei City, Taiwan

<sup>2</sup>Dept. of Information Management, Chung Hua University, Hsin-Chu City, Taiwan

Keywords: Fuzzy Decision, Shadow Set, Background-Shadow Model.

Abstract: Automatic road segmentation plays an important role in many vision-based traffic applications. It provides a priori information for preventing the interferences of irrelevant objects, activities, and events that take place outside road areas. The proposed road segmentation method consists of four major steps: background-shadow model generation and updating, moving object detection and tracking, background pasting, and road location. The full road surface is finally recovered from the preliminary one using a progressive fuzzy-theoretic shadowed sets technique. A large number of video sequences of traffic scenes under various conditions have been employed to demonstrate the feasibility of the proposed road segmentation method.

## 1 INTRODUCTION

Roads are important objects for many applications, such as road maintenance and management (Ndoye *et al.*, 2011), transport planning, traffic monitoring and measurement, traffic accident and incident detection, car navigation, autonomous vehicles (Perez *et al.*, 2011), road following (Skog *et al.*, 2009), and driver assistance systems. Regardless of diverse applications, road segmentation methods can broadly be divided into two groups. One group (Alvarez *et al.*, 2008)(Chen *et al.*, 2010)(Chung *et al.*, 2004)(Ha *et al.*, 2009)(Ndoye *et al.*, 2011) is concerned with road localization in the images of static traffic scenes, and another group (Alvarez *et al.*, 2011)(Courbon *et al.*, 2009)(Obradovic *et al.*, 2008)(Perez *et al.*, 2011)(Skog *et al.*, 2009) is devoted to the road detection in the images of dynamic traffic scenes. The images of static scenes are provided by stationary cameras, whereas those of dynamic scenes are captured by movable cameras, e.g., the cameras mounted on moving vehicles or robots. The roads exhibiting in the images of dynamic scenes are typically narrow-ranged, right in front of the carriers, and close to the cameras.

Figure 1(a) shows some examples of such images. However, the roads presenting in the images of static scenes can be rather different in both shape and size due to large variations in elevation and viewing direction from camera to camera. Figure 1(b) shows some images of static traffic scenes. The road

detection techniques developed for the images of static and dynamic scenes can be considerably different. In this study, we focus on the images of static traffic scenes, which are commonly considered in such applications as restricted lane monitoring, wide-area traffic surveillance, traffic parameter measurement, traffic accident/incident detection, and traffic law enforcement.

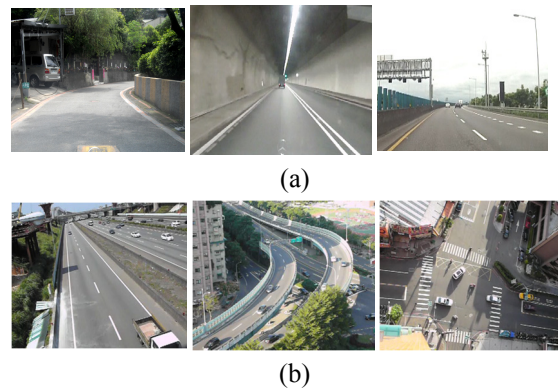


Figure 1: Example images of (a) dynamic traffic scenes and (b) static traffic scenes.

Road segmentation has often been modeled as a classification problem, in which image pixels are categorized as either road or non-road points based on their properties. The properties utilized have been ranging from the low-level ones (e.g., intensity, color, and depth) (Danescu *et al.*, 1994)(Santos *et al.*, 2013)(Tan *et al.*, 2006)(Sha *et al.*, 2007), the mid-level ones (e.g., texture, edge, corner, and surface

patch) (Santos *et al.*, 2013)(Soquet *et al.*, 2007), to the high-level ones (e.g., lane markings (Wang *et al.*, 2004), road boundaries, and road vanishing point) (Alvarez *et al.*, 2008). Various techniques characterized by different levels of pixel properties have been developed.

There have been a large number of different techniques proposed, such as deformable templates (Ma *et al.*, 2000), watershed transformation (Beucher *et al.*, 1994), morphological operations (Bilodeau *et al.*, 1992), V-disparity algorithm (Soquet *et al.*, 2007), probabilistic models (Danescu *et al.*, 1994), boosting (Santos *et al.*, 2013)(Fritsch *et al.*, 2014), and neural networks (Mackeown *et al.*, 1994). However, currently available road segmentation methods either dealt with the images of dynamic traffic scenes for such applications as car navigation, autonomous vehicles and driver assistance systems or considered the images of static traffic scenes of particular road types captured by cameras with specific elevations and viewing directions. In this paper, we present a general road segmentation technique applicable to the traffic images containing roads of various types, shapes and sizes under diverse weather (e.g., clear, cloudy, and rain days), illumination (e.g., sunlight and shadow), and environmental (e.g., traffic jams and cluttered backgrounds) conditions.

The proposed method consists of four major steps: background-shadow model generation and updating, moving object detection and tracking, background pasting, and road localization. In terms of these four steps, our contributions are addressed below. First, we model the road segmentation problem as a classification problem. The performance of classification heavily relies on the quality of the given road characteristics. In the background pasting step, a method of calculating road characteristics from reliably located road surfaces is presented. Second, it is inevitable that uncertainties originating from noise, errors, imprecision, and vagueness are involved throughout the entire process. We employed shadowed sets, which are extended from fuzzy sets that have been well known to be an elegant tool for coping with vague notions, to resolve uncertainties in the final step of road localization.

The rest of this paper is organized as follows. Section 2 addresses the overall idea of the proposed road segmentation method. Section 3 details the main steps of the proposed method. Experimental results are then demonstrated in Section 4. Conclusions and future work are finally given in Section 5.

## 2 AUTOMATIC ROAD SEGMENTATION

Figure 2 shows a block diagram for the proposed road segmentation method, in which four major steps are involved: (1) background-shadow model generation and updating, (2) moving object detection and tracking, (3) background pasting, and (4) road location. The details of these four steps are discussed in the next section. In this section, the basic idea and novelty of the proposed method is addressed.

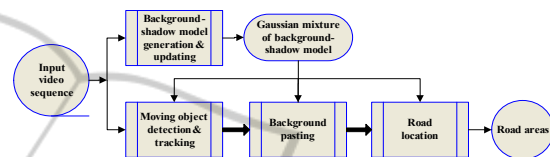


Figure 2: Block diagram for automatic road segmentation.

Let us look at an example shown in Figure 3 for illustrating the proposed method. Giving a video sequence of a traffic scene (Figure 3(a)), our ultimate goal is to locate the road areas of the scene (Figure 3(f)) in the video sequence. First of all, a background-shadow model of the scene is created from the input video sequence. This model contains both the background and shadow information of the scene in one model. Figure 3(b) shows a background image of the scene provided by the model. The model is then updated as time goes. This completes the step of background-shadow model generation and updating. Thereafter, moving objects are detected and tracked over the video sequence. Figure 3(c) shows the detected objects at a certain instant in time. Note that most of uninteresting moving

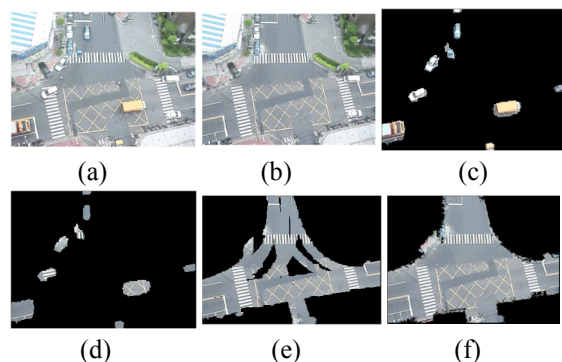


Figure 3: An example for illustrating the road segmentation process: (a) the traffic scene under consideration, (b) a background image of the scene, (c) the moving objects detected at a certain time instant, (d) the background patches corresponding to the detected moving objects, (e) a preliminary road segment, and (f) the recovered full road surface of the scene.

objects, such as flipping leaves and grasses, waving flags, flashing lights, and the shadows accompanying moving objects can be ignored because they have been regarded as background objects during building the background-shadow model. Ideally, only moving vehicles are located in the step of moving object detection and tracking. However, this is usually not the case. The subsequent steps will compensate for to some extent this drawback.

Moving vehicles are assumed to run on the road surface. Accordingly, the patches in the background image, called the background patches, that correspond to the moving objects are then extracted and pasted on a map, called the road map, shown in Figure 3(d). Repeating the steps of moving vehicle detection and background pasting, a preliminary road segment will eventually be established in the road map depicted in Figure 3(e). This preliminary road segment is inevitably error prone because of imperfect moving vehicle detection. We hence associate each pixel of the preliminary road segment with a degree of importance that is proportional to the times of applying background pasting to the pixel. Statistically, noisy pixels are random in nature and will have small degrees of importance. In the final step of road location, the preliminary road segment with its degrees of importance of pixels then serves as a seed, from which the full road region of the scene is progressively recovered by iteratively adding background pixels to the preliminary road segment based on both the proximities and affinities of the pixels to the preliminary road segment. Figure 3(f) shows the recovered road surface of the scene.

### 3 IMPLEMENTATIONS OF MAJOR STEPS

In this section, the four major steps: (1) background-shadow model generation and updating, (2) moving object detection and tracking, (3) background pasting, and (4) road location, involved in the proposed road segmentation method are detailed.

#### 3.1 Background-shadow Model Generation and Updating

A In the step of background-shadow model generation and updating, a Gaussian mixture background-shadow (GMBS) model (Wang *et al.*, 2011) of the traffic scene is created, which integrates

both the background and shadow information of the scene in one model. The reason we generate such a model is twofold. First, shadows often confuse our vehicle detection in view that they distort vehicle shapes and may connect multiple vehicles into one. Second, shadow detection is a complex and time-consuming process. Instead of applying shadow detection to every video image, we preserve in advance shadow information in the GMBS model so that we can rapidly identify shadows in images simply relying on the shadow information provided by the GMBS model.

#### 3.2 Moving Object Detection and Tracking

An approach combining the temporal differencing and the level set techniques is employed to detect moving objects in video sequences (Wang *et al.*, 2008). Temporal differencing locates the image areas that have significant changes in characteristic between successive images. Since the time interval between two successive video images is extremely short, it is reasonable to assume that the two images have been taken under the same illumination condition.

The level set technique (Paragios, 2006) provides a robust method to locate objects based on their edges even though involving imperfections. To use this technique, the initial contours of objects have to be provided. We group edges according to their closeness in both distance and property (i.e., edge magnitude) into clusters. Recall that an object may be contained in a single component or in a number of adjacent components in component image  $C'$ . The level set method then progressively moves the contour toward the edges inside the contour with a speed function in a direction normal to itself. The contour will eventually enclose the object when it firmly hits the edges of the object.

The above moving object detection procedure is somehow time consuming primarily due to the level set process that is iterative in nature. We introduce an object tracking process realized by the mean shift technique (Comaniciu *et al.*, 2003) to reduce the number of object detections. Once a moving object is detected, its subsequent locations are predicted by the object tracking process. For each prediction, the object detection process confirms it within the vicinity of the predicted location. Such a cooperation of location prediction and confirmation has significantly expedited the moving object detection and tracking step.

### 3.3 Background Pasting

In the background pasting step, the background patches corresponding to detected moving objects are pasted on an image, called the road map. Initially, road regions grow rapidly in the road image. The growth will gradually slow down until no obvious change is observed. A preliminary road segment can be attained. In general, the preliminary road segment contains several regions with different characteristics, e.g., asphalt pavements, lane marks, repaired road patches, and shadows falling on road surfaces.

We group the image pixels of the preliminary road segment into clusters, each of which contains pixels having similar characteristics, using the fuzzy c-means technique (Chen *et al.*, 1997). Small clusters are first ignored because they may result from noises. Recall that each pixel of the preliminary road segment possesses a degree of importance that is proportional to the number of moving vehicles passing through the pixel. We then compute the degrees of importance for the clusters based on those associated with their constituting pixels. We remove the clusters with small degrees of importance. These clusters may result from the perspective projections of large vehicles outside of the road region. Thereafter, for each remaining cluster its mean of characteristics of image pixels is calculated. Let  $\{m_1, m_2, \dots, m_c\}$  be the means of clusters, in which  $c$  is the number of clusters. Finally, we compute the chamfer distances  $D$  of image pixels from the preliminary road segment. Figure 4 shows an example of the above processing.

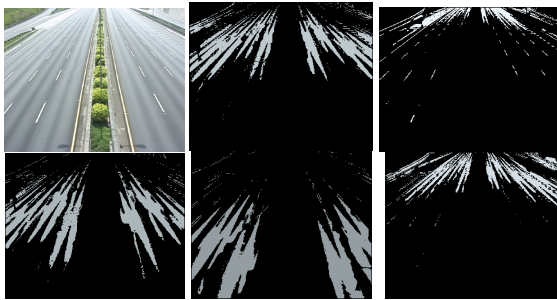


Figure 4: Five major clusters of homogeneous regions included in the preliminary road segment of Video 1. The top left is the background image and the others are homogeneous regions.

### 3.4 Road Location

In the road location step, the full road region is progressively recovered from the preliminary road segment. Figure 5 gives the algorithm of road

location. In each iteration, the degree  $\mu(x)$  of any image pixel  $x$  belonging to a road surface is first estimated based on both its characteristic  $a(x)$  and chamfer distance  $D(x)$ , i.e.,

$$\mu(x) = wg_1(\min_{1 \leq k \leq c} \|a(x) - m_k\|) + (1-w)g_2(D(x)), \quad (4)$$

where  $m_k$  is the mean vector of cluster  $k$ ,  $g_i(\cdot)$  ( $i = 1, 2$ ) are Gaussian functions, and  $w$  is a weighting factor for balancing image characteristic and chamfer distance. The above equation states that the more comparable the characteristic of the pixel to that of any cluster and that the closer the pixel to the preliminary road segment the larger the degree of the pixel belonging to a road surface. The characteristics  $a(x)$  and  $m_k$  are color vectors in our experiments.

Having determined the membership grades of pixels belonging to road surfaces, instead of simply selecting a constant threshold for the membership grades, we introduce the fuzzy theoretic shadowed set approach (Pedrycz, 2009) to automatically determine a threshold for separating image pixels into road and non-road pixels. Unlike fuzzy sets that describe vague concepts in terms of precise membership functions ( $F: X \rightarrow [0, 1]$ ), shadowed sets model vagueness with non-numeric models ( $S: X \rightarrow \{0, [ , 1], 1\}$ ). Function  $S$  possesses limited three-valued characterization and separates the universal set  $X$  into three subsets  $S_0, S_1$ , and  $S_{[ , 1]}$ . In other words, shadowed sets capture the essence of fuzzy sets at the same time reducing the numeric burden.

**Algorithm: Road Location**

Input:  $D$ : Chamfer distance of preliminary road segmentation

$a(x)$ : Characteristic of image pixel  $x$

$\{m_1, m_2, \dots, m_c\}$ : Means of characteristic of clusters

Steps:

1.  $w \leftarrow 0$

2. Computing degree of pixel  $x$  belong to a road surface using

$$\mu(x) = wg_1(\min_{1 \leq k \leq c} \|a(x) - m_k\|) + (1-w)g_2(D(x))$$

3. Computing threshold using

$$\alpha^* = \arg \min_{\alpha} \left| \sum_{\mu(x) \geq \alpha} \mu(x) + \sum_{\mu(x) \leq 1-\alpha} (1-\mu(x)) - \text{cardinality}\{x \mid \alpha < \mu(x) < 1-\alpha\} \right|$$

Selecting  $\alpha^*$  as the threshold of  $\mu(x)$  to classify pixel  $x$  into road and non-road points.

4. Increase  $w$  and repeat 2-4 until  $\alpha^*$  becomes increasing.

Figure 5: Algorithm for road location.

Let  $\alpha \in (0, 1/2)$  be an  $\alpha$ -cut of the membership function in Equation (4). Accordingly, three regions,

referred to as the rejected ( $\Omega_1 : \int_{x: \mu(x) \leq \alpha} \mu(x) dx$ ), marginal ( $\Omega_2 : \int_{x: \alpha < \mu(x) < 1-\alpha} 1 dx$ ), and fully accepted ( $\Omega_3 : \int_{x: \mu(x) \geq 1-\alpha} (1-\mu(x)) dx$ ) regions, can be defined.

Figure 6 shows an example membership function, from which the  $\Omega_1$ ,  $\Omega_2$ , and  $\Omega_3$  regions associated with a particular  $\alpha$ -cut  $\alpha$  are indicated. To condense uncertainty, it leads to the optimization problem of finding an  $\alpha$ -cut that best balances between the vagueness ( $\Omega_2$ ) and clearness ( $\Omega_1 + \Omega_3$ ) of the membership function, i.e.,

$$\alpha^* = \arg \min_{\alpha} |\Omega_1 + \Omega_3 - \Omega_2|$$

$$= \arg \min_{\alpha} \left| \int_{x: \mu(x) \leq \alpha} \mu(x) dx + \int_{x: \mu(x) \geq 1-\alpha} (1-\mu(x)) dx - \int_{x: \alpha < \mu(x) < 1-\alpha} 1 dx \right|$$

In the discrete case,

$$\alpha^* = \arg \min_{\alpha} \left| \sum_{\mu(x) \leq \alpha} \mu(x) + \sum_{\mu(x) \geq 1-\alpha} (1-\mu(x)) - \text{cardinal}\{x | \alpha < \mu(x) < 1-\alpha\} \right|$$

We then select  $\alpha^*$  as the threshold of the membership grades of image pixels to classify them into road and non-road points.

The above process repeats for different  $w$  values. We start with  $w = 0$ , i.e., the definition of membership grade  $\mu(x)$  of the image pixel at  $x$  completely depends on its chamfer distance  $D(x)$ . Thereafter,  $w$  progressively increases, i.e., increasing the influence

of the image characteristic  $a(x)$  of the pixel. In the beginning,  $\alpha$ -cut decreases as  $w$  increases. We terminate the road location step right before  $\alpha$ -cut becomes increasing. This is because we have empirically observed that  $\alpha$ -cut is closely related to an error rate of road segmentation we defined.

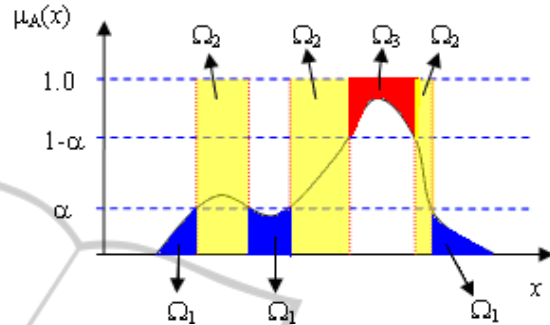


Figure 6: A shadowed set induced from a fuzzy set.

#### 4 EXPERIMENTAL RESULTS

A number of videos taken under various conditions of weather, illumination, viewpoint, road type, and congestion have been employed for experiments. Videos were acquired using a camcorder that provides 30 images of size 320 by 240 per second. No particular specification about the installation of the camcorder has been imposed. The lengths of

Table 1: Experimental results of demonstrative videos.

Video	Scene	Ground truth	Extracted road surface	Video	Scene	Ground truth	Extracted road surface
1				7			
2				8			
3				9			
4				10			
5				11			
6				12			
				13			

videos range from 2 to 3 minutes. Our algorithm written in C++ running on a PC at the rate of 2.5Hz takes about 30 to 150 seconds to complete the road segmentation of a video. The processing time depends on the complexities of both traffic and scene. Specifically, a slowly moving traffic needs a longer time to build the GMBS model of the scene.

A scene comprising a large portion of road surface will take time to locate moving objects for generating a preliminary road segment. In this study, we pay more attention on efficacy than efficiency.

Table 1 collects the input data, the intermediate and final results of some experimental videos. We refer to these videos as demonstrative videos from now on. The scenes, from which the videos are acquired, are depicted in the second column of the table. The third column shows the background images generated from the GMBS models of the scenes. We extract by hand from the background images the road surfaces for serving as ground truths displayed in the fourth column. The last two columns demonstrate the intermediate and final results of preliminary road segment as well as extracted road surface, respectively. The landscapes of the demonstrative videos include freeways (Videos 1 and 2), expressways (Videos 3 and 4), thoroughfares (Videos 5 and 6), streets (Videos 7 and 8), intersections (Videos 9 and 13), suburban road (Video 10), campus road (Video 11), and mountain road (Video 12). In addition to distinct road types, the demonstrative videos have been involved different conditions of illumination (daylight, sunshine and shadow), weather (sunny, cloudy and rainy days), congestion (rush and off-peak hours), and viewing direction.

To evaluate the performance of the proposed road segmentation method, we define the error rate  $\varepsilon$  of road segmentation as follows. The symbols  $N$ ,  $N_g$ ,  $N_e$ ,  $n_g$ , and  $n_e$ , they specify the numbers of pixels of the road image, the ground truth, the extracted road surface, the extracted road surface in and not in the ground truth, respectively. Accordingly, the number of misclassified pixels that are road pixels (i.e., false negatives) is  $N_g - n_g$  and the number of misclassified pixels that are not road pixels (i.e., false positives) is  $N_e - n_e$ . The total number of misclassified pixels is hence  $(N_g - n_g) + (N_e - n_e) = N_g + N_e - 2n_g$ . We normalize this number with the size  $N$  of the road image to define error rate  $\varepsilon = \frac{N_g + N_e - 2n_g}{N}$ .

In the road location step, parameter  $w$  plays an important role in defining the membership grades of image pixels belonging to road surface (Equation 4). The larger the value, the more significant the image

characteristic and the less influential the chamfer distance in locating road surfaces. Table 2 shows the error rates  $\varepsilon$  of road segmentation of the demonstrative videos under different  $w$ . In this table, the minimum error rate is marked for each demonstrative video. The  $w$  values corresponding to the minimum error rates range from 0.2 to 0.35. This suggests that we may choose  $w$  within  $[.2-s, 0.35+s]$ , where  $s$  is a small value, instead of the entire range of  $[.2, 1]$ . Although the searching range of  $w$  has been greatly reduced, we still face the issue as to which  $w$  will lead to the minimum error rate of road segmentation due to the fact that we don't know the ground truth during processing.

Recall that for each  $w$  an  $\alpha$ -cut is determined for serving as the threshold of the membership degrees of image pixels belonging to road surfaces. Table 3 shows the  $\alpha$ -cuts of the demonstrative videos decided under different  $w$ . In this table, the minimum  $\alpha$ -cuts are marked as well. Surprisingly, they exactly correspond to the minimum error rates in Table 2. In other words, minimum  $\alpha$ -cuts can be indicative of minimum error rates. Moreover, the former are more reliable to identify than the latter. In our algorithm, the road location step terminates once the minimum  $\alpha$ -cut is observed.

Several factors have impacted on the performance of our road segmentation. Among these, the viewing direction of the camcorder may be the most critical one. In Table 2, the columns corresponding to Videos 5, 6, and 7 have considerably smaller error rates than the other columns. As we can see in Table 1, these videos were acquired by the camcorder with its viewing directions nearly perpendicular to the road surfaces, or equivalently the tilt angles of the camcorder close to 90 degrees. Moreover, the tilt angles of the camcorder increase from Video 5 to 7 and their corresponding minimum error rates decrease (7.8, 5.5, 4.7). In other words, the larger the tilt angle of the camcorder the lower the error rate of road segmentation. Seeing Video 10 in Table 1, it has the smallest tilt angle of the camcorder among the thirteen demonstrative videos and has a relatively high error rate (20.1). This is because vehicles captured by the camcorder with a small tilt angle will be more likely to occlude large areas outside the road.

In Table 2, the columns corresponding to Videos 3 and 4 have considerably larger error rates than the other columns. Taking look at the experimental results of these two videos in Table 1, both missed a large portion of road surface near the top of the road images. Our algorithm failed to detect moving objects present in the top rows of images because

Table 2: Error rates  $\varepsilon$  of road segmentation for the demonstrative videos under different  $w$ .

2	3	4	5	6	7	8	9	10	11	12	13
14.5	23.4	21.8	10.0	7.6	6.3	11.8	16.8	20.2	17.5	18.7	18.6
14.3	23.1	21.6	9.3	6.9	5.9	11.3	16.7	20.2	17.4	18.0	18.5
14.1	22.6	21.3	8.7	6.1	5.5	10.9	16.6	20.1	17.1	17.5	18.2
13.9	22.4	21.2	8.0	5.5	5.0	10.6	16.5	20.1	16.9	17.0	18.1
13.8	22.0	20.9	7.8	6.0	4.7	10.3	16.6	20.1	16.8	16.7	17.8
13.7	21.7	20.7	8.2	7.0	5.2	10.1	16.6	20.1	16.9	16.4	18.9
14.0	21.6	20.6	8.5	8.2	5.8	10.2	16.9	20.1	17.5	17.3	20.6
14.7	22.7	21.3	8.4	9.4	6.4	10.4	18.0	20.4	18.3	18.2	22.4
15.8	23.9	22.1	9.6	10.8	7.0	10.4	19.3	20.7	19.0	19.4	25.0
16.3	25.0	22.8	10.3	12.5	7.9	11.1	21.0	20.8	19.9	20.4	27.3

they are too small. Defective preliminary road segments could result in imperfect road segmentation. Likewise, if a road area has no vehicle passing through during constructing the preliminary road segment, an incomplete road surface may be extracted. In the suburban road of Video 10, only 6 vehicles passed by during taking the video for about three minutes. Moreover, none of these vehicles went through the road area close to the lower left corner of the road image. The same situation is also

observed in the campus road of Video 11, where only pedestrians and bicycles are allowed. Both kinds of the objects are small as well as slow. In these two cases, longer videos would somewhat compensate for the drawbacks.




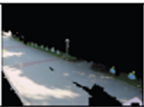



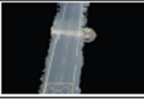


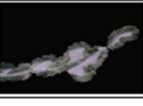

Another video sequence (Video 13) acquired in a rainy day has relatively large error rates, which are primarily resulting from the reflections of buildings on the road surface. The reflections of vehicles haven't caused troubles because vehicles are on the road. The reflections of buildings possess image characteristics similar to those of the actual buildings. The lower portions of the buildings besides the road will be regarded as road areas because they are close to the road area.

Finally, we compare the method proposed in this study with that previously reported in (Chung et al., 2004). Basically, the two methods consist of the same four major steps. However, the previous method has several weaknesses. First, the background model is generated using a progressively accumulating histogram approach. The generated background model cannot avoid regarding such moving objects as flipping leaves

Table 3:  $\alpha$ -cuts of the demonstrative videos under different  $w$ .

Video $w$	1	2	3	4	5	6	7	8	9	10	11	12	13
0.05	0.4	0.39	0.39	0.40	0.37	0.36	0.37	0.39	0.39	0.40	0.38	0.39	0.38
0.10	0.38	0.37	0.38	0.39	0.32	0.31	0.33	0.36	0.38	0.39	0.35	0.36	0.36
0.15	0.37	0.35	0.36	0.38	0.28	0.26	0.30	0.34	0.36	0.38	0.32	0.34	0.33
0.20	0.36	0.34	0.35	0.37	0.24	0.22	0.26	0.33	0.35	0.37	0.30	0.32	0.31
0.25	0.35	0.33	0.34	0.36	0.24	0.24	0.24	0.31	0.35	0.37	0.28	0.31	0.29
0.30	0.35	0.32	0.33	0.35	0.29	0.29	0.28	0.31	0.34	0.36	0.29	0.30	0.31
0.35	0.34	0.33	0.33	0.35	0.33	0.33	0.31	0.33	0.35	0.36	0.33	0.33	0.35
0.40	0.36	0.35	0.36	0.37	0.36	0.37	0.34	0.36	0.38	0.39	0.37	0.36	0.39
0.45	0.40	0.38	0.39	0.39	0.41	0.41	0.36	0.38	0.41	0.41	0.41	0.39	0.44
0.50	0.43	0.39	0.41	0.41	0.44	0.45	0.39	0.41	0.44	0.39	0.45	0.41	0.47

Table 4: Error rates  $\varepsilon$  of road segmentation for the previous and current methods.

	Video 1	Video 7	Video 10	Video 11	Video 12	Video 13
Previous method						
	$\varepsilon = 22.5\%$	5.7%	21.1%	11.7%	32.4%	18.2%
Current method						
	$\varepsilon = 10.1\%$	4.7%	20.1%	16.8%	16.4%	17.8%

and grasses, waving flags and flashing lights as foreground objects. Second, in the moving vehicle detection foreground objects are extracted simply using the background subtraction method. This method has suffered from illumination changes, especially shadows, as well as slowly moving traffics. Third, the morphological process ignores isolate road regions. This leads to defective preliminary road segments. Finally, there is no strategy for dealing with the problem of over-estimate due to perspective projection of vehicles moving along the roadside. The above drawbacks associated with the previous method have been compensated for in the current method. We have applied both the previous and current methods to all the 13 experimental videos. However, the previous method only worked on six of them (i.e., videos 1, 7, 10, 11, 12, and 13). This is probably because of the associated drawbacks mentioned above. Table 4 shows the experimental results, in which except for video 11, the current method has outperformed the previous one for the rest videos, especially videos 1 and 12.

## 5 CONCLUDING REMARKS AND FUTURE WORK

In this paper, an automatic road segmentation method was presented. The proposed method is dedicated to static traffic scenes. Previous researches have paid more attention on either dynamic or restricted static scenes. As a matter of fact, a large number of traffic applications have to do with static traffic scenes and various conditions of environment, weather, illumination, viewpoint, and road type can make the road segmentation of static traffic scenes challenging too. A number of video sequences of traffic scenes under different conditions have been used in our experiments. The error rates of road segmentation of all experimental videos were within 25%. In terms of potential applications, the performance of the proposed road segmentation method can be acceptable. We will keep improving the performance of the current method and develop potential applications in our future work

## REFERENCES

- Ndoye, M., Totten V. F., Krogmeier, J. V., and Bullock, D. M., 2011. Sensing and signal processing for vehicle re-identification and travel time estimation. *IEEE Trans. on Intelligent Transportation Systems*, 12(1), pp. 119-131.
- Perez, J., Milanés, V., and Onieva, E., 2011. Cascade architecture for lateral control in autonomous vehicles. *IEEE Trans. on Intelligent Transportation Systems*, 12(1), pp. 73-82.
- Skog, I., and P. Händel, 2009. In-car positioning and navigation technologies — A Survey. *IEEE Trans. on Intelligent Transportation Systems*, 10(3), pp. 4–21.
- Alvarez, J. M., Lopez, A., and Baldrich, R., 2008. Illuminant-invariant model-based road segmentation. *Proc. of IEEE Intelligent Vehicles Symp.*, Eindhoven University of Technology Eindhoven, The Netherlands.
- Chen, Y. Y., & Chen, S. W., 2010. A restricted bus-lane monitoring system. *Proc. of the 23rd IPPR Conf. on CVGIP*, Kaohsiung, Taiwan.
- Chung, Y. C., Wang, J. M., Chang, C. L., and Chen, S. W., 2004. Road segmentation with fuzzy and shadowed sets. *Proc. of Asian Conf. on Computer Vision*, Korea.
- Ha, D. M., Lee, J. M., and Kim, Y. D., 2004. Neural-edge-based vehicle detection and traffic parameter extraction. *Image and Vision Computing*, 22(11), pp.899-907.
- Alvarez, J. M. and Lopez, A. M., 2011. Road detection based on illumination invariance. *IEEE Trans. on Intelligent Transportation Systems*, 12(1), pp. 184-193.
- Courbon, J., Mezouar, Y., and Martinet, P., 2009. Autonomous navigation of vehicles from a visual memory using a generic camera model. *IEEE Trans. on Intelligent Transportation Systems*, 10(3), pp. 392-402.
- Obradovic, D., Lenz, H., and Shupfner, M., 2008. Fusion of sensor data in siemens car navigation system,” *IEEE Trans. on Vehicular Technology*, Vol. 56, No. 1, pp. 43-50, 2008.
- Danescu, R. and Nedeveschi, S., 1994. Probabilistic lane tracking in difficult road scenarios using stereovision. *IEEE Trans. on Intelligent Transportation Systems*, 10(2), pp. 272-282.
- Santos, M., Linder, M., Schnitman, L., Nunes, U., and Oliveria, L., 2013. Learning to segment roads for traffic analysis in urban images. *IEEE Intelligent Vehicles Symposium*, pp. 527-532, Gold Coast, QLD.
- Tan, C., Hong, T., Chang, T., and Shneier, M., 2006. Color model-based real-time learning for road following. *Proc. of the IEEE Conf. on Intelligent Transportation Systems*, Toronto, Canada.
- Sha, Y., Zhang, G. Y., and Yang, Y., 2007. A road detection algorithm by boosting using feature combination. *Proc. of IEEE Intelligent Vehicles Symposium*, Istanbul, Turkey.
- Wang, J. M., Chung, Y. C., Lin, S. C., Chang, S. L., and Chen, S. W., 2004. Vision-based traffic measurement system. *Proc. of IEEE Int'l. Conf. on Pattern Recognition*, Cambridge, United Kingdom.



- Wang, J. M., Chung, Y. C., Lin, S. C., Chang, S. L., and Chen, S. W., 2004. Vision-based traffic measurement system. *Proc. of IEEE Int'l. Conf. on Pattern Recognition*, Cambridge, United Kingdom.
- Ma, B., Lakshmanan, S., and Hero, A. O., 2000. Simultaneous detection of lane and pavement boundaries using model-based multisensor fusion," *IEEE Trans. on Intelligent Transportation Systems*, 1(3), pp. 135-147.
- Beucher, S. and Bilodeau, M., 1994. Road segmentation and obstacle detection by a fast watershed transform. *Proc. of the Intelligent Vehicles Symp.*, pp. 296-301.
- Bilodeau, M. and Peyrard, R., 1992. Multi-pipeline architecture for real time road segmentation by mathematical morphology," *Proc. of the 2nd Prometheus Workshop on Collision Avoidance*, pp. 208-214, Nurtlingen, RFA.
- Soquet, N., Aubert, D., and Hautiere, N., 2007. Road segmentation supervised by an extended V-disparity algorithm for autonomous navigation," *Proc. of IEEE Intelligent Vehicles Symp.*, Istanbul, Turkey.
- Mackeown, W. P. J., Greenway, P., Thomas, B. T., and Wright, W. A., 1994. Road recognition with a neural network. *Engineering Applications of Artificial Intelligence*, 7(2), pp. 169-176.
- Wang, J. M., Cherng, S., Fuh, C. S., and Chen, S. W., 2008. Foreground object detection using two successive images," *IEEE Int'l. Conf. on Advanced Video and Signal based Surveillance*, pp. 301-306.
- Paragios, N., 2006, Chapter 9: Curve Propagation, Level Set Methods and Grouping. *Handbook of Mathematical Models in Computer Vision*, Edited by N. Paragios, Y. Chen, and O. Faugeras, Springer Science + Business Media Inc., pp. 145-159.
- Comaniciu, D., Ramesh, V., and Meer, P., 2003. Kernel-based object tracking. *IEEE Trans. on Pattern Analysis and Machine Intelligence*, 25(5), pp. 564-577.
- Chen, S. W., Chen, C. F., Chen, M. S., Cherng, S., Fang, C. Y., and Chang, K. E., 1997. Neural-fuzzy classification for segmentation of remotely sensed images," *IEEE Trans. on Signal Processing*, 45(11), pp. 2639-2654.
- Pedrycz, W., 2009. From fuzzy sets to shadowed sets: interpretation and computing. *Int'l Journal of Intelligent Systems*, 24, pp. 48-61.
- Wang, J. M., Chen, S. W., and Fuh, C. S., 2011. Gaussian mixture of background and shadow model. *Proc. of the IADIS Conf. on Computer Graphics, Visualization, Computer Vision, and Image Processing*, Rome, Italy.
- Fritsch, J., Tobias, K., and Franz, K., 2014. Monocular road terrain detection by combining visual and spatial information. *IEEE Trans. on Intelligent Transportation Systems*, 15(4), pp. 1586-1596.